PHYSICAL REVIEW B VOLUME 22, NUMBER 5 1 SEPTEMBER 1980

Trapping of irradiation-induced defects by tin atoms in an Al-0.03 at.% Sn crystal

M. L. Swanson, L. M. Howe, and A. F. Quenneville
Atomic Energy of Canada Limited, Research Company, Chalk River Nuclear Laboratories, Chalk River, Ontario, Canada K0J 1J0
(Received 28 February 1980)

The backscattering-channeling method was used to investigate the trapping of irradiation-induced defects by Sn atoms in an Al-0.03 at.% Sn crystal. Since Sn atoms were not displaced appreciably from lattice sites by irradiation of the crystal at 35 or 70 K, or by subsequent annealing up to 160 K, it was concluded that mixed dumbbells were not formed by interstitial trapping in that temperature range. Further annealing up to 220 K produced a considerable displacement of Sn atoms from lattice sites. Channeling measurements along the ⟨110⟩, ⟨100⟩, and ⟨111⟩ axes indicated that the displaced Sn atoms were located in tetrahedral and octahedral interstitial sites. These displacements were attributed to multiple vacancy trapping at Sn atoms, because further irradiation at 70 K reduced the apparent displaced fraction of Sn atoms more than did irradiation at 35 K. Annealing at temperatures above 240 K caused a change in the Sn atom positions, indicating an alteration of the configuration of vacancy clusters.

I. INTRODUCTION

Most solute atoms trap self-interstitial atoms in metals.[1–7] Only in the case of solute atoms which are very similar in size and electronic properties to the host atoms, e.g., Ni atoms in Cu, may trapping be absent.[1,7] Several studies of the trapping properties of small solute atoms have been made using measurements of electrical resistivity,[5–7] Mössbauer effect,[8,9] internal friction,[10] diffuse x-ray scattering,[11] and ion channeling.[12–15] It has been shown[12–15] that such solutes trap self-interstitials in the mixed dumbbell configuration, which has a ⟨100⟩ orientation for face-centered-cubic crystals. This trapping configuration is stable up to stage III recovery (180–250 K in Al), where it annihilates with vacancies.

Large solute atoms appear to trap self-interstitials weakly,[4–7,13,16–18] and to release the self-interstitials during stage II recovery (50–180 K for Al). Channeling measurements have shown that the solute atoms are not displaced appreciably from lattice sites in these weak trapping configurations.[13,16] Thus the self-interstitials retain their normal configuration (presumably the ⟨100⟩ split interstitial for fcc metals) near a solute atom, in the manner envisaged by Hasiguti.[19]

From channeling measurements of irradiated metals, it has been found that large solute atoms, such as Sb, Ag, or Au atoms in Cu, or Sn atoms in Al, are displaced from lattice sites during stage III annealing.[12,16] It was suggested that the displacement of solutes in Cu was due to the trapping of several vacancies at each solute atom.[16] A multiple-vacancy-trapping model is required because the relaxation of a solute atom towards a single vacancy in fcc metals is not expected to be large enough to produce the observed channeling effects.[16,20] In the present experiments, the stage III displacement of Sn atoms following low-temperature He^+ irradiation and annealing of Al-0.03 at.% Sn crystals has been studied in some detail, in order to check the vacancy trapping model, and to specify the trapping configuration.

II. EXPERIMENTAL PROCEDURE

A single crystal of Al-0.03 at.% Sn was grown by the Bridgman method, annealed for 48 h at 873 K and then cooled slowly. Slices of this crystal were mechanically polished and electropolished to create a deformation-free surface region.[12] By varying the heat treatments of the slices, different substitutional fractions of Sn stoms could be obtained. (i) In slices of the as-cooled crystal, 50% of the Sn atoms were located on lattice sites. (ii) In slices which were annealed at 873 K for 600 s and then cooled rapidly under vacuum, about 80% of the Sn atoms were on lattice sites. (iii) In slices which were quenched from 873 K into water at 273 K, about 90% of the Sn atoms were on lattice sites.

The samples were irradiated and analyzed in the low-temperature target chamber of the 2.5-MV Chalk River Nuclear Laboratories Van de Graaff accelerator,[21] using 1-MeV He^+ ions. The sample temperature could be varied from 35 to 400 K, while a surrounding cryogenic shield was maintained at 20 K. For irradiations the ion beam was normally swept over a 0.050-cm^2 area, and the channeling analysis was done on a 0.010-cm^2 concentric area. The yields of backscattered He^+ ions were measured with a Si surface barrier detector at a scattering angle of 150°.

The position of solute atoms in a crystal is determined by measuring the normalized yields $\chi_i^{\langle lmn \rangle}$ and $\chi_h^{\langle lmn \rangle}$ of He^+ ions backscattered from solute and host atoms, respectively, for various ⟨lmn⟩ channels.[22–24] The apparent fraction of solute atoms which are dis-

 ©1980 The American Physical Society

placed from lattice sites into a given $\langle lmn \rangle$ channel is[22]

$$f_{di}^{\langle lmn \rangle} = (\chi_i^{\langle lmn \rangle} - \chi_h^{\langle lmn \rangle})/(1 - \chi_h^{\langle lmn \rangle}) \quad . \qquad (1)$$

Since the ion flux is not uniform across a channel, the actual displaced fraction is $f_{di}^{\langle lmn \rangle}/F_i^{\langle lmn \rangle}$, where $F_i^{\langle lmn \rangle}$ is the normalized ion flux at the position of the displaced solute atoms in the channel.[14] Because $F_i^{\langle lmn \rangle}$ is a calculated quantity which depends on the particular channeling and displacement models used, the empirical quantity $f_{di}^{\langle lmn \rangle}$ is conveniently used as a measure of solute atom displacements.[13–17, 22, 23] $F_i^{\langle lmn \rangle}$ has a value close to unity for displacements of about half the distance to the center of the channel. Near the center of a channel, $F_i^{\langle lmn \rangle}$ may approach a value of two, and near the edges of a channel it is less than unity. Precise determinations of solute atom displacements require detailed angular scans across several axial and planar channels.[23, 24]

Measurement of the irradiation-induced increase $\Delta(d\chi_h^{\langle lmn \rangle}/dz)$ in the dechanneling rate, where z is the depth, is a useful indication of the total concentration of lattice defects introduced by irradiation in metals.[12, 13, 23, 24] When this increase in dechanneling rate is reduced by annealing, it can be concluded that lattice defects have been annihilated. Thus changes in the position of solute atoms can be correlated with defect migration during annealing.

III. RESULTS

A. Displacement of Sn atoms during annealing

It was observed that 86–94% of the Sn atoms in water-quenched crystals of Al-0.03 at. % Sn were on substitutional lattice sites,[12] as can be seen from the data of Table I and the backscattering spectra of Fig. 1. Irradiation at 35–70 K with 1-MeV He^+ ions to

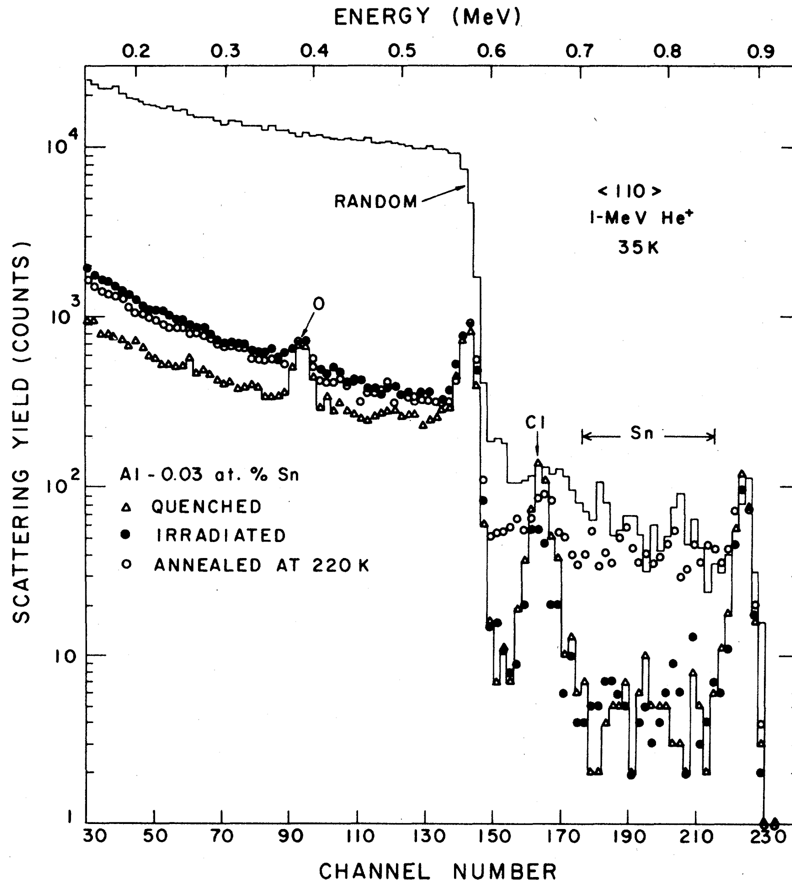

FIG. 1. Energy spectra of backscattered He^+ ions (initial energy 1 MeV) at 35 K for an Al-0.03 at.% Sn crystal which had been water quenched from 873 K (sample 6 of Table I). The $\langle 110 \rangle$ aligned spectra are shown before and after a random irradiation of 1-MeV He^+ ions at 35 K to a fluence of 1.0×10^{16} cm^{-2}, and after a subsequent 600-s anneal at 220 K. A spectrum for a random crystallographic direction, obtained by rotating the crystal, is also shown. The oxygen peak is the result of the thin surface layer of aluminum oxide. The chlorine peak is due to a surface residue left by the electropolishing solution. The energy window used in determining the yield of He ions backscattered from Sn atoms is indicated, and corresponds to a depth increment of 50–270 nm. This increment was used for yields from both Al and Sn atoms for all measurements in the present experiments.

TABLE I. Apparent displaced fraction of Sn atoms $f_{d\mathrm{Sn}}^{\langle lmn\rangle}$ [see Eq. (1)] in irradiated Al-0.03 at.% Sn crystals.

Sample	Irradiation fluence ϕ_R (10^{15} ions cm^{-2})	T_I [a] (K)	T_A [a] (K)	Alignment $\langle lmn\rangle$	$\chi_{\mathrm{Al}}^{\langle lmn\rangle}$	$\chi_{\mathrm{Sn}}^{\langle lmn\rangle}$	$f_{d\mathrm{Sn}}^{\langle lmm\rangle}$
1. Slow cooled	0	···	···	⟨110⟩	0.022	0.49	0.48
	13	40	···	⟨110⟩	0.065	0.53	0.50
			240	⟨110⟩	0.031	1.06	1.06
			240	{100}	0.382	0.930	0.89
			240	{111}	0.325	0.926	0.89
2. Slow cooled	0	···	···	⟨110⟩	0.020	0.510	0.50
	0	···	···	⟨111⟩	0.062	0.439	0.40
	23	35	···	⟨110⟩	0.047	0.456	0.43
		35	···	⟨111⟩	0.131	0.538	0.47
			240	⟨110⟩	0.030	1.038	1.04
			240	⟨111⟩	0.082	0.550	0.51
3. Vacuum quenched	0	···	···	⟨110⟩	0.029	0.230	0.21
	2.1[b]	40	···	⟨110⟩	0.034	0.247	0.22
			220	⟨110⟩	0.032	0.562	0.55
4. Water quenched	0	···	···	⟨110⟩	0.022	0.121	0.10
	0	···	···	{100}	0.270	0.35	0.11
	0	···	···	{111}	0.243	0.32	0.10
	4.1	70	220	⟨110⟩	0.029	0.45	0.43
		70	220	{100}	0.31	0.62	0.45
		70	220	{111}	0.24	0.60	0.47
		70	220	⟨111⟩	0.100	0.314	0.24
5. Water quenched	0	···	···	⟨110⟩	0.020	0.139	0.12
	0	···	···	⟨111⟩	0.071	0.154	0.09
	2.5[b]	70	···	⟨110⟩	0.028	0.172	0.15
		70	···	⟨111⟩	0.105	0.201	0.11
			247	⟨110⟩	0.027	0.46	0.45
			247	⟨111⟩	0.081	0.36	0.31
	2.5	40	···	⟨110⟩	0.035	0.22	0.19
			240	⟨110⟩	0.031	0.64	0.63
			240	⟨111⟩	0.100	0.44	0.38
	1.3	40	···	⟨110⟩	0.032	0.47	0.45
6. Water quenched	0	···	···	⟨110⟩	0.025	0.081	0.06
	0	···	···	⟨111⟩	0.070	0.112	0.05
	10	35	···	⟨110⟩	0.035	0.091	0.06
		35	···	⟨111⟩	0.101	0.158	0.06
			160	⟨110⟩	0.038	0.200	0.17
			160	⟨111⟩	0.100	0.201	0.11
			220	⟨110⟩	0.035	0.736	0.73
			220	⟨111⟩	0.087	0.315	0.25
			300	⟨110⟩	0.031	0.570	0.56
			300	⟨111⟩	0.080	0.589	0.55
			380	⟨110⟩	0.029	0.337	0.32
			380	⟨111⟩	0.076	0.419	0.37
7. Water quenched	0	···	···	⟨110⟩	0.032	0.166	0.14
	0	···	···	⟨100⟩	0.036	0.168	0.14
	0	···	···	⟨111⟩	0.070	0.172	0.11
	13	35	···	⟨110⟩	0.038	0.171	0.14
		35	···	⟨100⟩	0.055	0.201	0.15
		35	···	⟨111⟩	0.103	0.175	0.08
			220	⟨110⟩	0.034	0.960	0.96
			220	⟨100⟩	0.048	1.081	1.09
			220	⟨111⟩	0.081	0.346	0.29

[a] T_I and T_A were the temperatures of irradiation and of annealing (600-s pulses), respectively. The irradiations and anneals were performed sequentially *in situ* for each sample. All measurements were taken at 35–40 K. Typical statistical errors in $f_{d\mathrm{Sn}}^{\langle lmn\rangle}$ were ~ 0.02.

[b] With the exception of these irradiations, which were with 0.5-MeV He^{+}, all irradiations were with 1.0-MeV He^{+}. All analyses used 1.0-MeV He^{+}.

fluences up to $1.0\times10^{16}\text{cm}^{-2}$ did not affect $f_{d\mathrm{Sn}}^{\langle110\rangle}$, as shown in Fig. 1 and Table I (samples 5 to 7). However, subsequent annealing for 600 s at ~220 K caused $f_{d\mathrm{Sn}}^{\langle110\rangle}$ to increase by a large amount. For the sample shown in Fig. 1, this anneal increased $f_{d\mathrm{Sn}}^{\langle110\rangle}$ from 0.06 to 0.73; that is, the backscattering yield from Sn atoms approached the random level. Similar irradiation and annealing effects were observed for all slow cooled and quenched samples (Table I).

Detailed annealing results for irradiated Al-0.03 at. % Sn crystals are shown in Figs. 2 and 3. The data for quenched crystals showed a marked increase in the apparent displaced fraction $f_{d\mathrm{Sn}}^{\langle110\rangle}$ of Sn atoms during isochronal annealing between 180 and 220 K. In the same temperature range, it is seen that only about 50% of the irradiation-induced dechanneling increment annealed out. In contrast, it was shown previously for Al alloys containing small solute atoms that mixed dumbbells were created (i.e., $f_{di}^{\langle110\rangle}$ was increased) by interstitial trapping during 70-K irradiation and were completely annihilated, together with all of the irradiation-induced dechanneling increment, near 200 K.[12,13]

A notable feature of the annealing effect near 200 K, as shown in Fig. 3, was that the increase in $f_{d\mathrm{Sn}}^{\langle110\rangle}$ was much greater than the increase in $f_{d\mathrm{Sn}}^{\langle111\rangle}$, thus indicating preferential lattice positions of the displaced Sn atoms. However, during further annealing up to 300 K, the values of $f_{d\mathrm{Sn}}^{\langle110\rangle}$ and $f_{d\mathrm{Sn}}^{\langle111\rangle}$ became equal, while further recovery of the irradiation-induced dechanneling increment occurred.

During annealing from 300–400 K for the sample 6 of Fig. 3, $f_{d\mathrm{Sn}}^{\langle110\rangle}$ and $f_{d\mathrm{Sn}}^{\langle111\rangle}$ both decreased, and

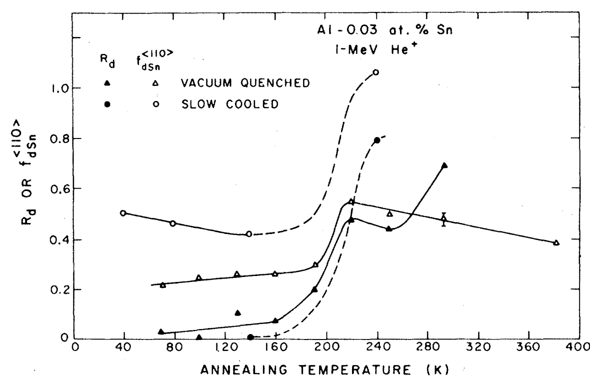

FIG. 2. Isochronal annealing (600-s pulse anneals) of a slow cooled and a vacuum quenched Al-0.03 at. % Sn crystal after irradiations as shown for samples 1 and 3, respectively, of Table I. All measurements were made at 40 K. The effect of annealing on both $f_{d\mathrm{Sn}}^{\langle110\rangle}$ and the recovery R_d of the irradiation-induced dechanneling increment is shown. The latter is defined as $R_d=1-\Delta(d\chi_{\mathrm{Al}}^{\langle110\rangle}/dz)/\Delta(d\chi_{\mathrm{Al}}^{\langle110\rangle}/dz)_{\max}$, where $\Delta(d\chi_{\mathrm{Al}}^{\langle110\rangle}/dz)_{\max}$ is the maximum increase in dechanneling rate caused by the irradiation.

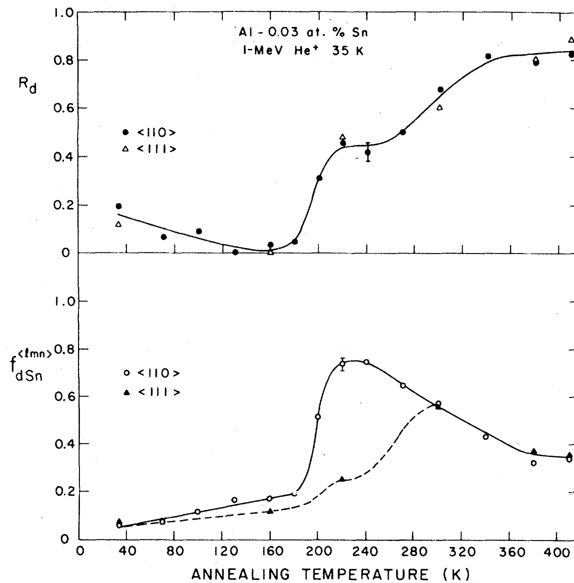

FIG. 3. Isochronal annealing (600-s pulse anneals) of a water quenched Al-0.03 at. % Sn crystal after irradiation with 1-MeV He ions at 35 K to a fluence of 1.0×10^{16} cm^{-2} (sample 6, Table I). In the lower part of the figure, the effect of annealing on $f_{d\mathrm{Sn}}^{\langle110\rangle}$ and $f_{d\mathrm{Sn}}^{\langle111\rangle}$ is shown. In the upper part, the recovery R_d of the irradiation-induced dechanneling increment is shown (see Fig. 2).

remained approximately equal, while there was little change in the rate of dechanneling. After the 400-K anneal, measurements on an unirradiated part of the crystal showed that some Sn precipitation had occurred, as $f_{d\mathrm{Sn}}^{\langle110\rangle}=0.27$. Thus the Sn displacements caused by the irradiation plus annealing treatments had almost completely disappeared by 400 K.

B. Lattice location of Sn Atoms

Angular scans through ⟨110⟩ and ⟨111⟩ axial channels of a slow-cooled crystal are shown in Figs. 4 and 5. The ⟨110⟩ angular scan (Fig. 4) was started at the perfectly aligned position, so as to avoid radiation damage. However, as shown by the data points taken after the ⟨111⟩ angular scan of Fig. 5, no significant difference in the Sn yields near ⟨110⟩ alignment was produced by the large irradiation at 35 K used for the ⟨111⟩ scan. The irradiation used for the ⟨110⟩ angular scan was equivalent to a random fluence of 8.5×10^{15} cm^{-2} and the total irradiation for both angular scans was equivalent to 2.3×10^{16} cm^{-2}. (In this case, the damage was introduced by the angular scans only, on an area identical to that used for subsequent channeling analysis.) Before and during these scans, $f_{d\mathrm{Sn}}^{\langle110\rangle}\simeq f_{d\mathrm{Sn}}^{\langle111\rangle}=0.45\pm0.05$. No structure was seen in the angular scan yields, indicating

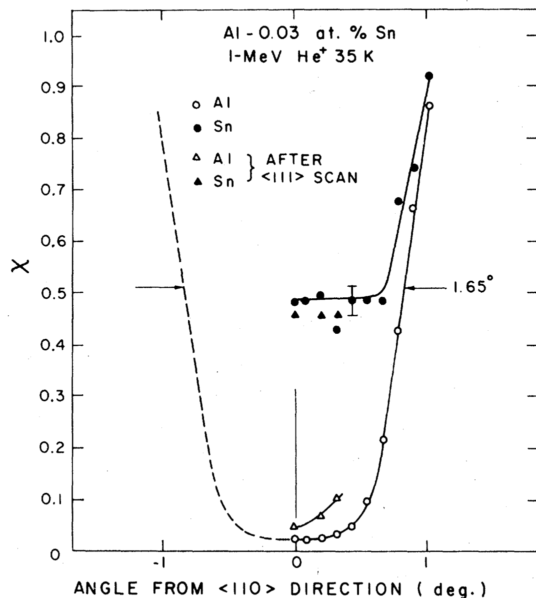

FIG. 4. Angular dependence of the normalized backscattering yields χ of 1-MeV He ions from Al and Sn atoms in a slow-cooled Al-0.03 at.% Sn crystal at 35 K. Following the $\langle 111 \rangle$ angular scan of Fig. 5, additional measurements were taken near the $\langle 110 \rangle$ aligned position, as shown. The yields were measured for a depth increment of 50–270 nm.

random positions of the displaced Sn atoms.

The crystal was then annealed for 600 s at 240 K and another $\langle 110 \rangle$ angular scan was performed at 35 K (Fig. 6). After this anneal, $f_{d\mathrm{Sn}}^{\langle 110 \rangle}$ had increased to 1.0 and was susceptible to reduction by subsequent 35-K irradiation (see Table I and Sec. III C). Thus

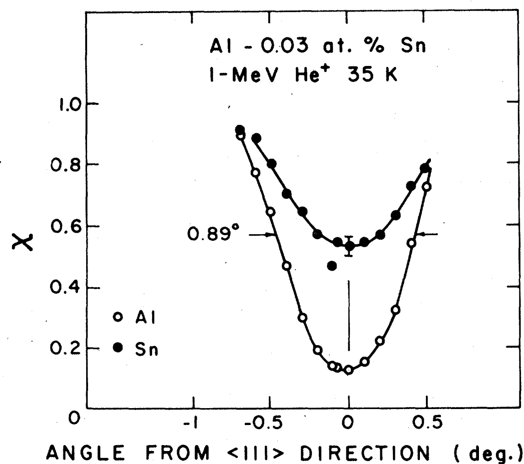

FIG. 5. Angular dependence of the normalized backscattering yields χ of 1-MeV He ions from Al and Sn atoms in a slow-cooled Al-0.03 at.% Sn crystal at 35 K, following the initial angular scan of Fig. 4.

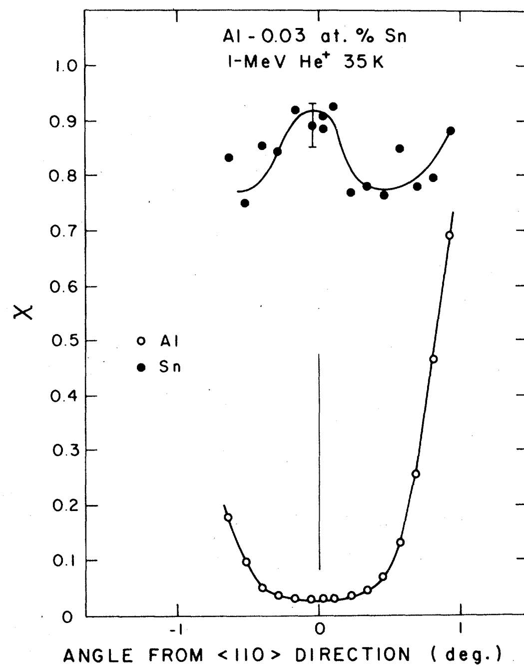

FIG. 6. Angular dependence of the normalized backscattering yields χ of 1-MeV He ions from Al and Sn atoms in a slow-cooled Al-0.03 at.% Sn crystal at 35 K, after the angular scans of Figs. 4 and 5 plus a 600-s anneal at 240 K (sample 2, Table I). The equivalent random fluence given the sample by the previous angular scans was 2.3×10^{16} cm^{-2}. The four points furthest from the $\langle 110 \rangle$ direction were measured last (two on either side). The Sn curve was drawn to guide the eye.

the angular scan was done only over the central part of the dip. A clear maximum in yield from the Sn atoms is seen, indicating that the Sn atoms had been displaced well towards the center of the $\langle 110 \rangle$ channel.[12,14,23,24]

The value of $f_{d\mathrm{Sn}}^{\langle 111 \rangle}$ was not appreciably altered by the low-temperature irradiation or by the subsequent 240-K anneal (sample 2, Table I). Thus in this case, annealing the irradiated crystal at 240 K caused the Sn atoms to be displaced into lattice positions which were completely shadowed in $\langle 111 \rangle$ channels. The body-centered position satisfied these requirements of peaking in $\langle 110 \rangle$ yields and shadowing in $\langle 111 \rangle$ channels.

For quenched samples, as shown in Table I and Fig. 3, not only $f_{d\mathrm{Sn}}^{\langle 110 \rangle}$, but also $f_{d\mathrm{Sn}}^{\langle 111 \rangle}$ was increased by annealing at $\sim$240 K after a low-temperature irradiation. However, in all cases $f_{d\mathrm{Sn}}^{\langle 111 \rangle}$ was less than $f_{d\mathrm{Sn}}^{\langle 110 \rangle}$, after annealing at 220–240 K, so that displacement of Sn atoms towards body-centered positions occurred. Further annealing above 240 K caused this inequality to vanish, as discussed in the previous section.

Angular scans through $\langle 100 \rangle$ and $\langle 110 \rangle$ axial

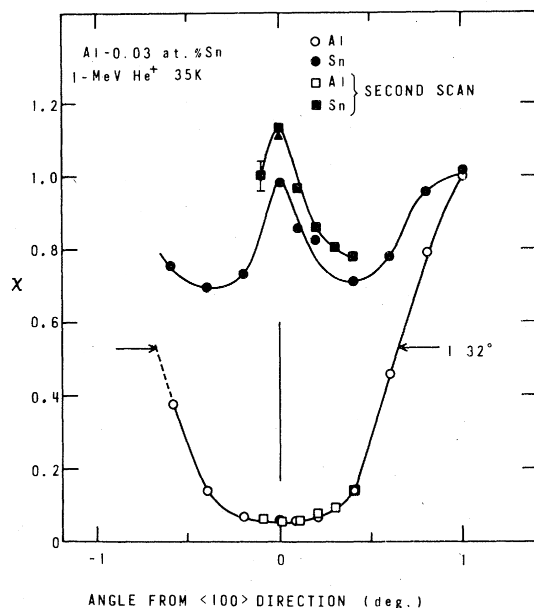

FIG. 7. Angular dependence of the normalized backscattering yields χ of 1-MeV He ions from Al and Sn atoms near a ⟨100⟩ direction for sample 7 of Table I, after the anneal at 220 K. Following the first angular scan, the sample was annealed again at 220 K for 600 s and a second partial angular scan was performed. The triangular symbol represents the Sn yield before these angular scans.

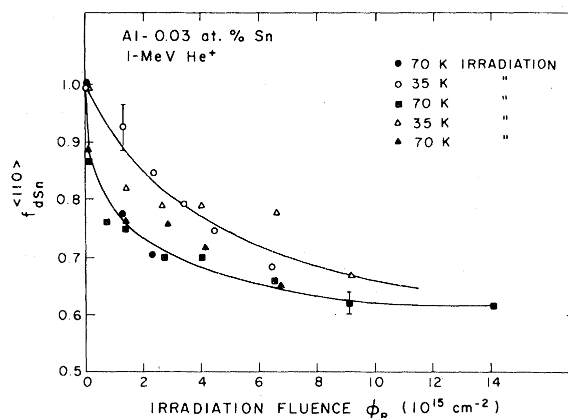

FIG. 8. Effect of irradiation fluence at 35 or 70 K (in a random crystallographic direction) on the apparent displaced fraction $f_{dSn}^{\langle 110 \rangle}$ of Sn atoms in a Al-0.03 at.% Sn crystal. Prior to the first set of irradiations at 70 K, the sample had been annealed at 240 K for 600 s following the angular scans of Figs. 4–6. Between each set of irradiations, the sample was annealed for 600 s at 240 K. The irradiations are listed in the order of measurement. The equivalent random fluence of the analyzing irradiations was included (Ref. 25).

channels were also measured for a water-quenched sample which had been irradiated with 1-MeV He^+ to a fluence of 1.3×10^{16} cm^{-2} at 35 K and then annealed 600 s at 220 K (sample 7, Table I). The ⟨100⟩ scans (Fig. 7) showed even stronger peaking in Sn yield than the ⟨110⟩ scan of Fig. 6. Since the first ⟨100⟩ angular scan was started at an angle of -0.6°, where χ_{Al} was appreciable (χ denotes the normalized backscattering yield) some depression of the Sn yield was observed because of the damage introduced by the analysis. Consequently, the crystal was annealed for 600 s at 220 K and a second partial scan near the ⟨100⟩ direction was performed, as shown in Fig. 7. The ⟨110⟩ angular scan (not shown) was similar to that of Fig. 6.

C. Reduction of Sn atom displacements by low-temperature irradiation

In crystals irradiated at 35–70 K, it was shown in Sec. III A that $f_{dSn}^{\langle 110 \rangle}$ was increased by annealing at 220–240 K. However, $f_{dSn}^{\langle 110 \rangle}$ was reduced by subsequent irradiation at 35–70 K (Table I). This effect is shown in Fig. 8 for the slow-cooled sample of Figs. 4–6. After the sample had been annealed at 240 K following the angular scans of Figs. 4–6, a series of irradiations at 35 or 70 K were performed. After each set of irradiations, the sample was annealed at 240 K. Each of these anneals restored the value of $f_{dSn}^{\langle 110 \rangle}$ to a high value between 0.90 and 1.0. Although there is considerable scatter in the experimental data of Fig. 8, it is clear that the rate of reduction in $f_{dSn}^{\langle 110 \rangle}$ was greater for irradiations at 70 than at 35 K.

D. Summary of results

The foregoing results, as well as data obtained for other slow-cooled and quenched crystals of Al-0.03 at.% Sn, shown in Table I, can be summarized as follows: (a) Since irradiation of Al-0.03 at.% Sn crystals at 35 to 70 K did not affect $f_{dSn}^{\langle 110 \rangle}$, $f_{dSn}^{\langle 100 \rangle}$, or $f_{dSn}^{\langle 111 \rangle}$, it is clear that the Sn atoms were not appreciably displaced from lattice sites in the temperature range (35–50 K) where self-interstitial Al atoms are mobile.[26,27] (b) Annealing of irradiated Al-0.03 at.% Sn crystals in the temperature range 180–240 K caused considerable displacement of Sn atoms into ⟨110⟩ and ⟨100⟩ channels. After this treatment, $f_{dSn}^{\langle 110 \rangle}$ and $f_{dSn}^{\langle 100 \rangle}$ were greater than $f_{dSn}^{\langle 111 \rangle}$. (c) Further annealing of irradiated crystals from 240–300 K caused a decrease in $f_{dSn}^{\langle 110 \rangle}$ and an increase in $f_{dSn}^{\langle 111 \rangle}$ until the two values became equal. (d) Following low-temperature irradiation plus annealing at 240 K, additional irradiation at 35–70 K caused a reduction in $f_{dSn}^{\langle 110 \rangle}$. The rate of decrease was greater for irradiations at 70 than at 35 K.

IV. DISCUSSION

A. Sn atom positions in unirradiated crystals

As shown in Table I, up to 94% of the Sn atoms in an Al-0.03 at.% Sn crystal can be retained in substitutional lattice sites by a rapid quench into water from a temperature of 873 K. In slow-cooled crystals, only 50% of the Sn atoms were on lattice sites. The remainder were presumably in the form of precipitates, as the values of $f_{d\mathrm{Sn}}^{\langle lmn\rangle}$ in $\langle 110\rangle$ and $\langle 111\rangle$ axial channels were similar, and irradiation did not alter these fractions. Also, the angular scans of Figs. 4 and 5 for a slow-cooled crystal indicated random positions of Sn atoms. Solubility data[28] are consistent with the existence of Sn precipitates in such alloys.

B. Trapping of Al self-interstitials by Sn atoms

It has been shown by several electrical resistivity and channeling measurements[4–7, 13, 16–18] that large solute atoms generally trap self-interstitial atoms weakly in fcc metals. The self-interstitials are released during annealing below 180 K. In dilute Al-Sn alloys which were irradiated at liquid-nitrogen temperature with fast neutrons,[29] a recovery stage in electrical resistivity, which was centered at 138 K, increased in magnitude with increasing Sn concentration, thus supporting the shallow-trapping model.

The present channeling results verify this model of interstitial trapping at Sn solute atoms in Al. As shown in Table I, irradiation of Al-0.03 at.% Sn crystals at 35–70 K did not appreciably displace Sn atoms into $\langle 110\rangle$, $\langle 100\rangle$, or $\langle 111\rangle$ channels. Thus, since Al self-interstitials are mobile in that temperature range[26, 27, 30] and are presumably trapped by Sn atoms, it follows that the trapping configuration is a shallow one rather than the mixed dumbbell (in which the solute atom is displaced a large distance from its lattice site). Furthermore, as shown in Figs. 2 and 3, the release of Al self-interstitials from Sn atoms near 138 K also did not affect $f_{d\mathrm{Sn}}^{\langle 110\rangle}$; this result indicates that deeper traps such as the mixed dumbbell were not created by annealing at more elevated temperatures (up to about 180 K).

C. Trapping of vacancies by Sn atoms during stage III recovery

The present results indicate strongly that the displacement of Sn atoms which was caused by stage III annealing (near 200 K) after low-temperature irradiation was due to multiple trapping of vacancies by Sn atoms. It is expected that the trapping of a single vacancy by a Sn atom would not displace the Sn atom more than 0.01 nm from a lattice site,[20] and this displacement is not sufficient to explain the observed large increase in $f_{d\mathrm{Sn}}^{\langle 110\rangle}$ and $f_{d\mathrm{Sn}}^{\langle 100\rangle}$. The main evidence which supports a vacancy-trapping model rather than an interstitial-trapping mechanism in stage III is the data of Fig. 8. The reduction in $f_{d\mathrm{Sn}}^{\langle 110\rangle}$ by irradiation at 35 or 70 K can be attributed to migration of self-interstitials to the defect clusters created by the stage III recovery. As the vacancy cluster size is reduced by the absorption of interstitials, a reduction in $f_{d\mathrm{Sn}}^{\langle 110\rangle}$ occurs. Furthermore, the rate of decrease of $f_{d\mathrm{Sn}}^{\langle 110\rangle}$ was greater for the 70-K irradiations, where interstitials are freely mobile, than for the 35-K irradiations, where the recovery stage I_D occurs.[27, 30] This recovery stage is peaked near 36 K, and is associated with correlated interstitial-vacancy recombination; that is, with short-range movement of Al interstitials to the vacant lattice sites from which they were ejected. Thus the probability that interstitials reach vacancy clusters is less during 35-K irradiations than during 70-K irradiations.

The present channeling results are similar to those obtained for dilute alloys of Cu containing 0.1 at.% of Au, Sb, or Ag, where solute atom displacement during stage III recovery was also attributed to vacancy clustering at the solute atoms.[16] In that case also the displaced fraction of solute atoms was reduced by subsequent low-temperature irradiations. However, no preferred lattice sites were observed for the displaced solute atoms, in contrast to the present results, as outlined in Sec. III B.

There is other considerable evidence for vacancy clustering at solute atoms in fcc metals during stage III recovery. The electrical resistivity data of Ceresara *et al.*,[29] previously referred to, showed that the presence of Sn solute atoms in neutron-irradiated Al caused the retardation of complete recovery well beyond stage III; that is, above 240 K. The emergence of a series of annealing peaks in the stage IV region for the Sn-doped Al was attributed to several different geometric combinations of the vacancies trapped at Sn atoms. This general conclusion was supported by previous precipitation and quenching data which showed that vacancies had a considerable binding energy to Sn atoms (0.2–0.4 eV).[31, 32] More recent hyperfine interaction data on quenched or irradiated Al containing small amounts of ^{111}In have demonstrated the trapping of vacancies by In atoms in the stage III recovery region (230 K).[33, 34] Perturbed angular correlation studies of ^{111}In which was implanted into Ni have indicated that two unique geometric configurations of In atoms surrounded by vacancies exist.[35] One configuration is possibly an In atom surrounded by three nearest-neighbor vacancies in a {111} plane.[36] It was proposed that the other configuration could be an In atom surrounded by a tetrahedron of four vacancies.[35] In irradiated or quenched Cu containing small amounts of ^{111}In, perturbed angular correlation measurements have indicated that two distinct kinds of vacancy trapping occur at In atoms during stage III recovery (near 260 K).[37] Detailed positron annihilation studies of the

trapping of vacancies by Sb atoms in plastically deformed Ni have also indicated that multiple trapping of vacancies by the Sb atoms occurred during annealing in the stage III region, in this case above 350 K.[38]

D. Vacancy-Sn atom trapping configurations

In the previous section, it was concluded that the displacement of Sn atoms from lattice sites in irradiated Al-0.03 at.% Sn crystals, which occurred during stage III recovery, was due to clustering of vacancies at the Sn atoms. It was shown in Sec. III B that the Sn atoms in these clusters were displaced further into ⟨110⟩ and ⟨100⟩ channels than into ⟨111⟩ channels. The maxima in backscattering yields from Sn atoms which occurred at both ⟨110⟩ and ⟨100⟩ directions (Figs. 6 and 7), can be explained by Sn atoms being displaced into both octahedral (body-centered) and tetrahedral lattice sites. For octahedral sites, the calculated[14] normalized ion flux $F_i^{\langle 110\rangle} \simeq 2.3$ and $F_i^{\langle 100\rangle} = 0$, whereas for tetrahedral sites, $F_i^{\langle 110\rangle} \simeq 1.0$ and $F_i^{\langle 100\rangle} \simeq 2.5$. For both of these sites, $F_i^{\langle 111\rangle} = 0$. Thus, the present data for sample 7 after the anneal at 220 K are consistent with approximately 25% of Sn atoms in substitutional lattice sites, 30% in random interstitial sites, 30% in tetrahedral sites, and 15% in octahedral sites. The Sn atoms in tetrahedral and octahedral sites could be surrounded by 4 and 6 vacancies, respectively. The configuration involving a Sn atom situated in the center of a triangle of nearest-neighbor vacancies[36] may also be present.

The existence of certain geometric configurations of vacancies surrounding Sn atoms is consistent with the varied experiments cited in the previous section.[29,33–38] The observed change in defect configuration which occurred on annealing the present samples above 240 K, as shown by the altered ratio of $f_{d\text{Sn}}^{\langle 110\rangle} / f_{d\text{Sn}}^{\langle 111\rangle}$, is also in agreement with the results quoted previously.

The present results demonstrate that ion channeling is a very promising method for studying the geometric configurations of vacancies trapped at solute atoms. In the case of Sn solutes in Al, multiple trapping of vacancies caused Sn atoms to be displaced into tetrahedral and octahedral interstitial sites.

ACKNOWLEDGMENTS

The authors would like to thank J. Lori and G. R. Bellavance for technical assistance and I. V. Mitchell for comments on the manuscript.

[1] T. H. Blewitt, R. R. Coltman, C. E. Klabunde, and T. S. Noggle, J. Appl. Phys. 28, 639 (1957).
[2] A. Sosin and H. H. Neely, Phys. Rev. 127, 1465 (1972).
[3] A. Sosin, in *Lattice Defects and Their Interactions*, edited by R. R. Hasiguti (Gordon and Breach, New York, 1967), p. 235.
[4] C. P. Cannon and A. Sosin, Radiat. Eff. 25, 253 (1975).
[5] A. Kraut, F. Dworschak, and H. Wollenberger, Phys. Status Solidi B 44, 805 (1971).
[6] F. Dworschak, A. Kraut, K. Sonnenberg, and H. Wollenberger, Radiat. Eff. 19, 119 (1973).
[7] H. Wollenberger, J. Nucl. Mater. 69–70, 362 (1978).
[8] G. Vogl, W. Mansel, and W. Vogl, J. Phys. F 4, 2321(1974).
[9] W. Mansel and G. Vogl, J. Phys. F 7, 253 (1977).
[10] L. E. Rehn, K.-H. Robrock, and H. Jacques, J. Phys. F 8, 1835 (1978).
[11] C. B. Larson and H.-G. Haubold, J. Nucl. Mater. 69–70, 758 (1978).
[12] M. L. Swanson and F. Maury, Can. J. Phys. 53, 1117(1975).
[13] M. L. Swanson, L. M. Howe, and A. F. Quenneville, J. Nucl. Mater. 69–70, 372 (1978).
[14] N. Matsunami, M. L. Swanson, and L. M. Howe, Can. J. Phys. 56, 1057 (1978).
[15] L. M. Howe, M. L. Swanson, and A. F. Quenneville, J. Nucl. Mater. 69–70, 744 (1978).
[16] M. L. Swanson, L. M. Howe, and A. F. Quenneville, Radiat. Eff. 28, 205 (1976).
[17] M. L. Swanson, L. M. Howe, and A. F. Quenneville, J. Phys. F 6, 1629 (1976).
[18] C. Dimitrov, F. Moreau, and O. Dimitrov, J. Phys. F 5, 385 (1975).
[19] R. R. Hasiguti, J. Phys. Soc. Jpn. 15, 1807 (1960).
[20] A. C. Damask and G. J. Dienes, *Point Defects in Metals* (Gordon and Breach, New York, 1963).
[21] J. Bøttiger, J. A. Davies, J. Lori, and J. L. Whitton, Nucl. Instrum. Methods 109, 579 (1973).
[22] M. L. Swanson, L. M. Howe, and A. F. Quenneville, Phys. Status Solidi A 31, 675 (1975).
[23] S. T. Picraux, *New Uses of Low Energy Accelerators*, edited by J. F. Ziegler (Plenum, New York, 1975), p. 229.
[24] D. S. Gemmell, Rev. Mod. Phys. 46, 129 (1974).
[25] M. L. Swanson, P. Offermann, and K. H. Ecker, Can. J. Phys. 57, 457 (1979).
[26] W. Schilling, J. Nucl. Mater. 69–70, 465 (1978).
[27] W. Schilling, G. Burger, K. Isebeck, and H. Wenzl, *Vacancies and Interstitials in Metals* (North-Holland, Amsterdam, 1970), p. 255.
[28] M. Hansen, *Constitution of Binary Alloys* (McGraw-Hill, New York, 1958).
[29] S. Ceresara, T. Federighi, and F. Pieragostini, Philos. Mag. 10, 893 (1964).
[30] C. Dimitrov, O. Dimitrov, and F. Dworschak, J. Phys. F 8, 1031 (1978).
[31] H. Kimura and R. R. Hasiguti, J. Phys. Soc. Jpn. 18, Suppl. III, 73 (1963).
[32] A. J. Perry and K. M. Entwistle, J. Inst. Met. 96, 344 (1968).
[33] H. Rinneberg and H. Haas, Hyper. Inter. 4, 678 (1978).
[34] H. Rinneberg, W. Semmler, and G. Antesberger, Phys. Lett. A 66, 57 (1978).
[35] C. Hohenemser, A. R. Arends, H. de Waard, H. G. Devare, F. Pleiter, and S. A. Drentje, Hyper. Inter. 3, 297 (1977).
[36] F. Pleiter, Hyper. Inter. 4, 710 (1978).
[37] Th. Wichert, M. Deicher, O. Echt, and E. Recknagel, Phys. Rev. Lett. 41, 1659 (1978).
[38] G. Dlubek, O. Brümmer, N. Meyendorf, P. Hautojärvi, A. Vehanen, and J. Yli-Kauppila, J. Phys. F 9, 1961 (1979).